

Ab initio study of Curie temperatures of diluted III-V magnetic semiconductors

J. Kudrnovský^{1,4}, I. Turek^{2,3,4}, V. Drchal^{1,4}, J. Mašek¹, F. Máca^{1,4}, and P. Weinberger⁴

¹ *Institute of Physics, Academy of Sciences of the Czech Republic,
Na Slovance 2, CZ-182 21 Prague 8, Czech Republic*

² *Institute of Physics of Materials, Academy of Sciences of the Czech Republic,
Žižkova 22, CZ-616 62 Brno, Czech Republic*

³ *Department of Electronic Structures, Charles University, Ke Karlovu 5,
CZ-121 16 Prague, Czech Republic*

⁴ *Center for Computational Materials Science, Technical University of Vienna,
Getreidemarkt 9, A-1060 Vienna, Austria*

Abstract

The electronic structure of diluted (Ga,Mn)As magnetic semiconductors in the presence of As-antisites and magnetic disorder is studied within the framework of the local spin density approximation. Both the chemical and magnetic disorders are treated using the coherent potential approximation. A ground state with partial disorder in the local moments and with a reduced total magnetic moment appears in the presence of As-antisites. We first estimate the Curie temperature T_c from total energy differences between the ferromagnetic and the paramagnetic state by identifying these with the corresponding energy difference in a classical Heisenberg model. A more systematic approach within the framework of the mean-field approximation to estimate T_c consists in an evaluation of the effective exchange fields acting on the magnetic moment at a given site. The presence of As-antisites strongly reduces the Curie temperature. The results indicate that the effect of impurities on the

electronic structure cannot be neglected and influences the Curie temperature non-negligibly. A comparison of the calculated Curie temperatures to existing experimental data indicates an increase of the donor concentration with the increase of the Mn-content.

PACS numbers: 71.15.Nc, 71.20.Nr, 75.30.Et, 75.50.Pp

I. INTRODUCTION

Because of their ferromagnetic properties, diluted magnetic III-V semiconductors (DMS) represent a new class of materials with potential technological applications in spintronics [1]. The physics of DMS is in particular interesting because of the yet unclear origin of the occurring ferromagnetism and the even less understood role of disorder. It is now generally accepted that the ferromagnetic coupling in III-V DMS containing Mn impurities is mediated via valence band holes in the host semiconductor. Mn atoms that substitute three-valent cations in the host act as acceptors which in turn create holes in the valence band. For finite concentration of Mn atoms the Fermi energy is then pinned within the valence band. The ferromagnetic coupling of Mn atoms is often qualitatively explained by the fact that because of the small size of the corresponding hole Fermi surface the period of the Ruderman-Kittel-Kasuya-Yosida (RKKY) oscillations exceeds the typical distance between Mn atoms.

Theoretical approaches to the DMS can be divided into two groups, namely model studies using the effective-mass approximation, and studies based on the detailed knowledge of the electronic structure. The model studies mostly employ the kinetic-exchange model (KEM) in the connection with a continuum approximation for the distribution of Mn atoms and other defects [2,3], a model that yields a disorder-free problem, although it was recently refined in order to include disorder via a supercell method by means of Monte Carlo simulations [4,5]. A simpler model assuming that holes hop only between Mn-sites, where they interact with the Mn moments via phenomenological exchange interactions, was also developed [6].

Electronic structure studies based on the spin-density functional theory (DFT) in the framework of the local spin-density approximation (LSDA) represent a further step towards a more detailed, parameter-free description of the properties of DMS. One possibility of describing such system is a supercell approach [7–9], in which large cells are used to simulate semiconductor crystals with magnetic atoms and other impurities. The supercell approach has limited applicability because it leads to excessively large supercells for low concentrations of impurities characteristic for DMS. Alternatively, one can employ Green function methods

in which the configurational averaging is performed within the coherent potential approximation (CPA) [10] and the resulting averaged Green function can be used to determine any physical quantity of interest. The Green function approach can be implemented, e.g., in the framework of the Korringa-Kohn-Rostoker (KKR) method [11,12] or the tight-binding linear muffin-tin orbital method (TB-LMTO) [13] as in the present case. DMS with Curie temperatures (T_c) in the range of the room temperature are needed for practical applications; the study of realistic models for evaluation of T_c is thus of great importance. The evaluation of the Curie temperature on *ab initio* level is still a challenging task, in particular for complex alloy systems like the DMS. Conventional approaches known from model studies [2,3] cannot be directly employed for evaluation of T_c . Therefore, a different approach has to be adopted for the LSDA Hamiltonian. It is well-known [14] that transversal fluctuations of the local magnetization have to be taken into account to describe temperature-dependent properties of magnetic itinerant systems. The direct evaluation of the corresponding enhanced frequency-dependent magnetic susceptibility [15] is very complicated, in particular for such complex random systems like DMS. A tractable approach is based on the adiabatic treatment of atomic moments in which noncollinear configurations of magnetic moments are taken into account. The adiabatic approximation is well justified for magnetic atoms with large exchange splittings, like, e.g., Mn-atoms. This method can be implemented either in the real space [16–18] or in the reciprocal space (the frozen-magnon approach) [19]. The real-space approach can be naturally applied to random system in the framework of the CPA while in the reciprocal-space approach the supercell method has to be adopted [20].

In the real-space approach employed here the total energy is mapped onto a classical Heisenberg model whose statistical treatment represents a next step. The mapping is further simplified by using the magnetic force-theorem [16] which allows to use the band energy of the calculated ground state as a good estimate also for total-energy differences of the perturbed ground state. The separated treatment of statistical degrees of freedom is another advantage of this approach as it can be done on different levels of sophistication. It is one of the goals of the present paper to describe evaluation of the Curie temperature of DMS in the framework

of the above mentioned two-step model.

DMS containing Mn atoms, such as (Ga,Mn)As mixed crystals, are highly compensated systems. The experimentally observed number of holes in the valence band is much lower than the concentration of Mn-impurities and indicates the presence of other lattice defects acting as donors. The As-antisites, i.e., As atoms on the Ga-sublattice, add two electrons to the valence band for each defect compensating thus two holes. Interstitial Mn atoms acting as double donors have the same effect [9] as the As-antisites. Recent theoretical studies indicate that magnetic structures with partial disorder of local magnetic moments can lower the total energy of system as compared to the ferromagnetic state. The stability of the ferromagnetic state was studied in [5] within the KEM model concluding that non-collinear ferromagnetism is common in DMS. A new magnetic state stabilized by the As-antisites and characterized by a partial disorder in the orientations of the local Mn-magnetic moments was found recently also in first-principles studies of $\text{Ga}_{0.96}\text{Mn}_{0.04}\text{As}$ alloys [21]. All this indicates the great importance of various defects for the electronic structure, magnetic properties, and the Curie temperature of the DMS. A detailed understanding of such influence calls for a parameter-free approach. A detailed study of the influence of As-antisites is another goal of the present paper.

II. ELECTRONIC STRUCTURE

In this section we present results of electronic structure calculations, in particular the magnetic phase diagram, magnetic moments, and densities of states for the whole range of physically interesting concentrations of Mn-impurities and As-antisites.

A. Model and computational details

We have determined the electronic structure of DMS in the framework of the *ab initio* all-electron tight-binding linear muffin-tin orbital (TB-LMTO) method within the atomic-sphere approximation [13]. The valence basis consists of *s*-, *p*-, and *d*-orbitals, we include

scalar-relativistic corrections but neglect the spin-orbit effects. The substitutional disorder due to Mn-atoms and As-antisites is treated in the CPA. Although the CPA neglects local environment effects and possible lattice relaxations it correctly reproduces concentration dependent trends and can also treat systems with small but finite concentrations of defects typical for DMS. We introduce empty spheres [22] into the interstitial positions of the zincblende GaAs semiconductor for a better space filling. The lattice constant of the pure GaAs ($a = 5.653 \text{ \AA}$) was used in all calculations but we have verified that we can neglect a weak dependence of the sample volume on defect concentrations. We used equal Wigner-Seitz radii for all atoms and empty spheres. Charge selfconsistency is achieved within the framework of the local spin density approximation using the Vosko-Wilk-Nusair parametrization for the exchange-correlation potential [23]. The details of the method can be found in Ref. [24].

In general, in addition to the chemical disorder, the DMS are characterized also by some degree of magnetic disorder. We treat this disorder in the framework of the disordered local moment (DLM) method [21,25,26] which is the simplest way of including disorder in spin orientations. The DLM can be included in the framework of the CPA: the Mn atoms have collinear but random positive (Mn^+) and negative (Mn^-) orientations. The corresponding concentrations, x^+ and x^- , fulfill the condition $x = x^+ + x^-$, where x is the total Mn-concentration. The degree of magnetic disorder can be characterized by the order parameter $r = (x^+ - x^-)/x$ which is directly related to the macroscopic magnetization. Clearly, $x^\pm = (1 \pm r)x/2$. The GaAs mixed crystal with prescribed concentrations of x Mn- and y As-atoms on the Ga-sublattice can thus be treated formally as a multicomponent $(\text{Ga}_{1-x-y}\text{Mn}_{(1+r)x/2}^+\text{Mn}_{(1-r)x/2}^-\text{As}_y)\text{As}$ alloy with a varying parameter r , $0 \leq r \leq 1$. In the saturated ferromagnetic (FM) state, $r = 1$, all magnetic moments are aligned in the direction of a global magnetization. The paramagnetic (PM) state, $r = 0$, is characterized by a complete disorder of spin directions with vanishing total magnetization. The magnetic state with $0 < r < 1$, the partial ferromagnetic (pFM) state, is characterized by some degree of disorder in the spin-orientations [21]. It should be noted that the DLM method is used here only to determine the corresponding ground magnetic state in the presence of

impurities. The Curie temperature is, however, determined from the Heisenberg Hamiltonian corresponding to a given magnetic ground state where fluctuations of local magnetization are taken into account.

B. Magnetic phase diagram

We have determined the order parameter r that corresponds to the ground state at $T = 0$ for the whole range of physically relevant concentrations (x, y) in steps of $\Delta x = 0.01$ and $\Delta y = 0.0025$. In order to find the order parameter r we varied for each composition (x, y) the ratio r in steps $\Delta r = 0.05$ and evaluated the corresponding total energy. The magnetic phase diagram determined in this way is presented in Fig. 1a. It should be noted that in addition to the FM and PM states there exist the pFM state with a certain degree of disorder in the spin-orientations. The pFM state, which separates the FM phase from the PM phase, appears in the concentration region where the number of holes is reduced by As-antisites ($y > 0$). Without As-antisites the ground state is the FM state. For $y > x/2$, i.e., in the n -type materials, we did not find any indication for an electron-induced ferromagnetism even at the highest studied concentrations of donors. Further details can be read off from Fig. 1b, in which for a fixed Mn concentration of $x = 0.05$ the total energy with respect to the ground state is displayed as a function of the order parameter r . For less than 1% of As-antisites the ground state is a saturated ferromagnet, for more than 2.35% of As-antisites a paramagnet, with a partial ferromagnet inbetween. Empty circles for $y=0.015$ in Fig. 1b denote results obtained for the experimental lattice constant of $(\text{Ga}_{0.95}\text{Mn}_{0.05})\text{As}$ alloy ($a = 5.672 \text{ \AA}$) and demonstrates that the ground state is not changed by a variation of the lattice constant.

C. Magnetic moments

The magnetic state of disordered magnetic semiconductors can be characterized by the local magnetic moment at the sites occupied by Mn atoms and by the total magnetic magnetization which involves both localized moments at magnetic impurities and the induced

moments at non-magnetic atoms. The calculations show that the total magnetic moment per unit cell is proportional to the concentration of Mn atoms. This is the reason why we consider the total magnetic moment normalized to one Mn atom.

The calculated total and the local Mn-magnetic moments for $(\text{Ga}_{0.95-y}\text{Mn}_{0.05}\text{As}_y)\text{As}$ are presented in Fig. 2 as a function of the concentration y of As-antisites. The size of the local moments on Mn atoms is almost independent of the chemical composition and depends only weakly on the direction of the moments. This justifies, *a posteriori*, the validity of the DLM model in the present case [25,26].

The total magnetic moment per Mn-atom equals to $4 \mu_B$ in the system without As-antisites. The integer value of the moment is a consequence of the half-metallic character of the system. It is in agreement with the expectation that the localized moment of $5 \mu_B$ combines with the opposite moment of one hole in the majority-spin valence band. The difference between total and local moments shows the degree of the magnetic polarization of the host material. Although the induced moments on non-magnetic atoms are generally very small, they add to a non-negligible contribution to the total magnetic moment.

In systems with compensating impurities, the total magnetic moment per Mn-atom increases linearly with y and extrapolates to the value of $5 \mu_B$ in the completely compensated ferromagnetic state. In reality, however, this situation is not reached because the transition from the FM to the pFM state takes place at $y \approx 0.01$. The transition is marked by a drop of the magnetization in the total magnetic moment for $y > 0.01$. The reason for the decrease of the magnetization in the pFM state is obvious: the averaged local moment on Mn atoms, $m^{\text{Mn}} = x^+ m^{\text{Mn}^+} + x^- m^{\text{Mn}^-}$, is strongly reduced in the presence of Mn-sites with reversed moments. Clearly, the induced part of the magnetization also decreases proportionally to m^{Mn} .

D. Densities of states

The total density of states (DOS) per unit cell and the local Mn-density of states for $(\text{Ga}_{0.95}\text{Mn}_{0.05})\text{As}$ in the FM state are presented in Fig. 3. We find a good agreement with existing results (see, e.g., Ref. [12]). In addition, we present the Mn-local DOS on the Ga-sublattice resolved with respect to orbital symmetries. The different behavior of t_2 - and e -states which are split due to the tetragonal environment is clearly seen. The t_2 -states just above the top of the GaAs host valence band were experimentally observed [8,27]. The influence of As-antisites is illustrated in Fig. 4. We have chosen $y = 0.015$, i.e., the ground state is the pFM state with a partial disorder in local moments (see Fig. 1a). The local Mn^+ -DOS is quite similar to that in Fig. 3 because $x^+ \approx 0.044$. On the contrary, the local Mn^- -DOS exhibits a sharp peak which is characteristic for a single-impurity limit ($x^- \approx 0.006$). Such behavior also qualitatively explains the stability of the FM phase for systems without As-antisites: the Fermi energy in the pFM state without antisites, i.e., with larger number of holes in the valence band, would be shifted downwards and would be situated within a sharp peak of the minority Mn^- states which is energetically unfavorable.

III. CURIE TEMPERATURE

In this section we present two different ways of evaluating the mean-field Curie temperature using the selfconsistent DFT calculations. They are both implicitly based on the classical Heisenberg model, however, without the need for an explicit evaluation of the corresponding pair exchange interactions.

A. Simple estimate of the Curie temperature

A simple estimate of T_c can be obtained from DFT calculations by relating T_c to the total energy difference per unit cell between the paramagnetic and the ferromagnetic state as obtained from selfconsistent calculations, i.e., $\Delta = E_{\text{PM}} - E_{\text{FM}}$. The DFT describes

only the ground state properties, therefore an additional procedure is needed to estimate T_c . The classical Heisenberg model $H = - \sum_{i \neq j} J_{ij} \mathbf{e}_i \cdot \mathbf{e}_j$, where \mathbf{e}_i and \mathbf{e}_j are unit vectors characterizing the orientations of the local magnetic moments at sites i and j , and the J_{ij} denote the effective exchange interactions between a pair of magnetic atoms, provides a suitable tool to describe magnetic properties at finite temperatures. We can identify Δ with the energy resulting from a classical Heisenberg model since the corresponding energies in the FM and PM states are given by $E_{\text{FM}} = -x^2 \sum_{i \neq 0} J_{0i}^{\text{Mn,Mn}}$ and $E_{\text{PM}} = 0$, respectively. $J_{0i}^{\text{Mn,Mn}}$ denote the exchange interactions between Mn-atoms and all other interactions are neglected. On the other hand, the mean-field theory of the classical Heisenberg model yields $k_{\text{B}}\tilde{T}_c = 2x \sum_{i \neq 0} J_{0i}^{\text{Mn,Mn}}/3$, so that we have the following simple estimate,

$$k_{\text{B}}\tilde{T}_c = 2\Delta/3x. \quad (1)$$

It should be noted that non-magnetic As-antisites influence the Curie temperature only indirectly via Δ , which depends on the concentrations x and y of Mn-atoms and As-antisites, respectively.

B. Effective on-site exchange parameters

A more systematic approach to the evaluation of T_c was developed by Liechtenstein and coworkers [16] and it is based on the evaluation of magnetic excitation energies from the ground state which are mapped onto the effective Heisenberg Hamiltonian. The Curie temperature is then obtained from its consequent statistical study. A simpler approach, which avoids the direct evaluation of exchange interactions, consists in the determination of the effective exchange field acting on the magnetic moment at this site. From this field the Curie temperature is estimated using the generalized molecular field theory [16,17]. In the framework of the mean-field approximation adopted here are both approaches equivalent [16], but the latter one is much simpler when applied to complex systems with few sublattices. Recently, we have applied this approach to evaluate Curie temperatures of bulk ferromagnets

[17] as well as low-dimensional systems such as ultrathin films [18] and achieved a good agreement with available experimental data.

The basic quantity needed for a determination of T_c is the effective on-site exchange parameter for Mn-atoms, \bar{J}_i^{Mn} , which represents the Weiss field acting on site i . In the framework of the TB-LMTO approach we obtain [16,17]

$$\bar{J}_i^{\text{Mn}} = -\frac{1}{4\pi} \text{Im} \int_C \text{tr}_L \left[\delta_i^{\text{Mn}}(z) (\bar{g}_{ii}^{\text{Mn},\uparrow}(z) - \bar{g}_{ii}^{\text{Mn},\downarrow}(z)) + \delta_i^{\text{Mn}}(z) \bar{g}_{ii}^{\text{Mn},\uparrow}(z) \delta_i^{\text{Mn}}(z) \bar{g}_{ii}^{\text{Mn},\downarrow}(z) \right] dz. \quad (2)$$

Here tr_L denotes the trace over angular momenta $L = (\ell m)$, the energy integration is performed in the upper half of the complex energy plane over a contour C starting below the bottom of the valence band and ending at the Fermi energy, and $\delta_i^{\text{Mn}}(z) = P_i^{\text{Mn},\uparrow}(z) - P_i^{\text{Mn},\downarrow}(z)$, where $P_i^{\text{Mn},\sigma}(z)$ are the L -diagonal potential functions of Mn atoms corresponding to the spin-index σ ($\sigma = \uparrow, \downarrow$). The quantity $\delta_i^{\text{Mn}}(z)$ is proportional to the corresponding exchange splitting. Finally, the quantities $\bar{g}_{ii}^{\text{Mn},\sigma}(z)$ refer to site-diagonal blocks of the conditionally averaged Green function, namely, the average of the Green function over all configurations with a Mn-atom fixed at the site i [24]. The quantity \bar{J}_i^{Mn} reflects the details of the electronic and lattice structures of the system, its carrier concentration, as well as the effect of various kinds of impurities on the resulting electronic structure. The mean-field value of the Curie temperature is given by

$$k_B T_c = \frac{2}{3} \bar{J}_i^{\text{Mn}}. \quad (3)$$

The effective on-site exchange parameters corresponding to non-magnetic atoms are at least two-orders of magnitude smaller than \bar{J}_i^{Mn} . In Table I we compare \bar{T}_c calculated from expressions (1) and (3): both approaches give similar values.

A general trend of Curie temperatures in the FM phase as a function of the chemical composition (x, y) is illustrated in Fig. 5. T_c increases with x in systems without As-antisites and reaches the room temperature at approximately $x = 0.05$ and then decreases. The same trend and similar values of T_c were obtained recently in the framework of the frozen-magnon

approach applied to large ordered supercells [20]. The Curie temperature for a fixed Mn-concentration is strongly reduced with increasing concentration of As-antisites. This result clearly indicates a strong correlation between T_c and the number of carriers known also from model studies [2,27]. Detailed results for $(\text{Ga}_{1-x-y}\text{Mn}_x\text{As}_y)\text{As}$ alloys without ($y = 0.0$) and with ($y = 0.01$) As-antisites are presented in Fig. 6a. In both cases T_c saturates for higher Mn-concentrations which in turn indicates that the effective exchange interactions $\bar{J}_{0i}^{\text{Mn,Mn}}$ should decrease with increasing Mn doping. For $y = 0.01$ the Curie temperature is reduced by approximately 100 K–150 K over the whole range of Mn-concentrations as compared to the case of $y = 0.0$; the results are in a reasonably good agreement with experimental data for ferromagnetic metallic samples ($0.035 < x < 0.055$) [1].

The concentration of As-antisites y in Mn-enriched samples is not well known from the experiment [1]. The detailed knowledge of T_c as a function of x and y , Fig. 5, allows to make an estimate of the relation between x and y in such systems. We have inserted the experimental points into Fig. 5: for each experimental T_c corresponding to a given x we have determined the concentration y such that the calculated and experimental [1] Curie temperatures coincide. Points obtained in this way follow approximately a straight line. This allows to make an important conclusion, namely that the number of As-antisites increases with the concentration of Mn-atoms. A recent evaluation of the formation energy of the As-antisite defect in GaMnAs [28] confirms this conclusion.

The dependence of T_c on the concentration of As-antisites for a fixed Mn-concentration is presented in Fig. 6b. Full circles correspond to the FM state. There is a monotonic decrease of T_c with increasing y due to the decreasing number of holes in the valence band which mediate the ferromagnetic coupling between Mn atoms. This result is in a qualitative agreement with predictions of the KEM model [2,3,27]. In the present case, however, the concentration of holes is not a free parameter but it is given by the chemical composition (x, y) . We have also determined T_c for the pFM state which is the ground state for $y > 0.011$ (see Fig. 1b). We have now two magnetic atoms Mn^+ and Mn^- , but the Curie temperature T_c can be still estimated from Eq. (3). It should be noted that now the larger of the

two values $\bar{J}_i^{\text{Mn}^\pm}$ has to be inserted in (3) since the magnetism of such alloy is dominated by this constituent [29] (empty circles). The transition between the FM and pFM states is manifested by the change of the slope of the curve (see also Fig. 2). The regions of parameters for which the ferromagnetic, partial ferromagnetic, and paramagnetic phases exist are also shown. It should be noted that in the pFM case the Curie temperature is shifted to higher values of y than in the FM phase.

C. Effect of disorder on Curie temperature

Further we investigate the effect of disorder, neglected in the framework of the KEM, on the Curie temperature. For $(\text{Ga}_{0.95-y}\text{Mn}_{0.05}\text{As}_y)\text{As}$ alloys with constant Mn content is the effect of impurities in the framework of the KEM reduced simply to the change of the number of carriers. The present theory includes the effect of disorder on the electronic structure and hence also on T_c in the framework of the CPA. The Curie temperature is influenced by disorder via quantities $\bar{g}_{ii}^{\text{Mn},\sigma}(z)$ in Eq. (2) which depend on the varying concentration of Mn-atoms and As-antisites. We will demonstrate that the effect of disorder on T_c is non-negligible.

To this end we have evaluated the Curie temperature as a function of the number of holes in the valence band while keeping the same reference density of states, i.e., by employing the rigid-band model. All quantities in (2) correspond to the reference system but the Fermi energy is an adjustable parameter corresponding to a given alloy composition. The results are summarized in Table II assuming $(\text{Ga}_{0.95}\text{Mn}_{0.05})\text{As}$ as a reference system and are compared with selfconsistent calculations in which the effect of impurities is fully taken into account. We will first consider the effect of As-antisites assuming $(\text{Ga}_{0.95-y}\text{Mn}_{0.05}\text{As}_y)\text{As}$ alloys for which the number of holes in the valence band varies as $n_h = 0.05 - 2y$ while the concentration of Mn atoms is kept constant. The selfconsistent calculations and the rigid-band values follow the same trend but the latter ones are systematically smaller and quantitative differences increase with y : for $y = 0.005$ and $y = 0.01$ are the rigid-band values

88% and 62% of the selfconsistent ones, respectively.

It is also possible to use the same approach for estimating T_c for $(\text{Ga}_{1-x}\text{Mn}_x)\text{As}$ alloys without As-antisites. In this case, however, we have to scale the calculated rigid-band values in the spirit of the KEM model by a factor x_{ref}/x , where the reference Mn-concentration $x_{\text{ref}} = 0.05$. The results are similar to the previous case: we observe the same trends in both cases but the rigid-band values are lower than in the case in which the effect of disorder is fully taken into the account. We can conclude that the neglect of disorder does not change the qualitative trends of the calculated T_c as a function of Mn- and As-concentrations. On the other hand, the disorder leads in general to an enhancement of T_c as compared to the model in which the effect of disorder is treated approximately in the framework of the rigid-band model. This is not surprising as the rigid-band model is not able to describe properly the effect of As- and Mn-impurities which both represent a strong perturbation of the electronic structure.

IV. CONCLUSIONS

Based on first-principles calculations we have investigated the effect of As-antisites on the electronic and magnetic properties of $(\text{Ga},\text{Mn})\text{As}$ alloys. In addition to chemical disorder magnetic disorder was described using the disordered local moment model. Both the chemical and the magnetic disorder are treated within the framework of the coherent potential approximation. The mean-field Curie temperatures were estimated from the effective exchange fields acting on a given magnetic atom as well as from total energy differences between the ferromagnetic and paramagnetic state and showed a reasonable agreement between both approaches.

The main results can be summarized as follows: (i) there exists an additional phase with partially ordered local magnetic moments which separates the FM and PM states in the magnetic phase diagram. This phase is stabilized by As-antisites and has a reduced magnetization; (ii) our detailed study of the local magnetic moments justifies *a posteriori* the

validity of the disordered local moment model for determination of magnetic properties of DMS; (iii) a strong reduction of the Curie temperature occurs with increasing concentration of the As-antisites; (iv) with increasing concentration of Mn-atoms the calculations indicate a reduction of the exchange interactions between Mn atoms; (v) a comparison of the calculated and the measured concentration dependences of the Curie temperature indicates a correlation between the concentrations of Mn-impurities and As-antisites, namely an increase of the donor concentration with an increase of the Mn-content; and **(vi) a proper account of the influence of impurities on the electronic structure is needed for a quantitative estimate of the Curie temperature, in particular, the Curie temperature is reduced if the effect of disorder on the electronic structure is neglected.**

ACKNOWLEDGEMENTS

The financial support provided by the Grant Agency of the Czech Republic (No. 202/00/0122), the Grant Agency of the Academy of Sciences of the Czech Republic (No. A1010203, A1010214), the Czech Ministry of Education, Youth, and Sports (COST P5.30, MSM 113200002), the CMS Vienna (GZ 45.504), and the RTN *Computational Magnetoelectronics* (HPRN-CT-2000-00143) is gratefully acknowledged.

REFERENCES

- [1] H. Ohno, *Science* **281**, 951 (1998).
- [2] K. König, J. Schliemann, T. Jungwirth, and A.H. MacDonald, in *Electronic structure and magnetism in complex materials*, eds. D.J. Singh and D.A. Papaconstantopoulos (Springer-Verlag, Berlin, 2002).
- [3] T. Dietl, H. Ohno, and F. Matsukura, *Phys. Rev. B* **63**, 195205 (2001).
- [4] J. Schliemann, J. König, and A.H. MacDonald, *Phys. Rev. B* **64**, 165201 (2001);
C. Timm, F. Schäfer, and F. von Oppen, *Phys. Rev. Lett.* **89**, 137201 (2002).
- [5] J. Schliemann and A.H. MacDonald, *Phys. Rev. Lett.* **88**, 137201 (2002).
- [6] R.N. Bhatt and M. Berciu, *Phys. Rev. Lett.* **87**, 107203 (2001).
- [7] S. Sanvito, P. Ordejón, and N.A. Hill, *Phys. Rev. B* **65**, 165206 (2001).
- [8] M. van Schilfgaarde and O.N. Mryasov, *Phys. Rev. B* **63**, 233205 (2001).
- [9] J. Mašek and F. Máca, *Acta Phys. Polon. A* **100**, 319 (2001); F. Máca and J. Mašek,
Phys. Rev. B **65**, 235209 (2002).
- [10] B. Velický, H. Ehrenreich, and S. Kirkpatrick, *Phys. Rev.* **175**, 747 (1968).
- [11] H. Akai, *Phys. Rev. Lett.* **81**, 3002 (1998).
- [12] T.C. Schulthess and W.H. Butler, *J. Appl. Phys.* **89**, 7021 (2001).
- [13] O.K. Andersen and O. Jepsen, *Phys. Rev. Lett.* **53**, 2571 (1984).
- [14] T. Moriya, *Spin Fluctuations in Itinerant Electron Magnetism* (Springer, Berlin, 1985).
- [15] S.Y. Savrasov, *Phys. Rev. Lett.* **81**, 2570 (1998).
- [16] A.I. Liechtenstein, M.I. Katsnelson, V.P. Antropov, and V.A. Gubanov, *J. Magn. Magn. Mater.* **67**, 65 (1987); V.P. Antropov, B.N. Harmon, and A.N. Smirnov, *J. Magn. Magn. Mater.* **67**, 65 (1987).

- Mater. **200**, 148 (1999).
- [17] M. Pajda, J. Kudrnovský, I. Turek, V. Drchal, and P. Bruno, Phys. Rev. B **64**, 174402 (2001).
- [18] M. Pajda, J. Kudrnovský, I. Turek, V. Drchal, and P. Bruno, Phys. Rev. Lett. **85**, 5424 (2000).
- [19] S.V. Halilov, H. Eschrig, A.Y. Perlov, P.M. Oppeneer, Phys. Rev. B **58**, 293 (1998).
- [20] L.M. Sandratskii and P. Bruno, Phys. Rev. B **66**, 134435 (2002).
- [21] P.A. Korzhavyi, I.A. Abrikosov, E.A. Smirnova, L. Bergqvist, P. Mohn, R. Mathieu, P. Svedlindh, J. Sadowski, E.I. Isaev, Yu.Kh. Vekhilov, and O. Eriksson, Phys. Rev. Lett. **88**, 187202 (2002).
- [22] D. Glötzel, B. Segal, and O.K. Andersen, Solid State Commun. **36**, 403 (1980).
- [23] S.H. Vosko, L. Wilk, and M. Nusair, Can. J. Phys. **58**, 1200 (1980).
- [24] I. Turek, V. Drchal, J. Kudrnovský, M. Šob, and P. Weinberger, *Electronic Structure of Disordered Alloys, Surfaces and Interfaces*, (Kluwer, Boston, 1997); I. Turek, J. Kudrnovský, and V. Drchal, in *Electronic Structure and Physical Properties of Solids*, ed. H. Dreyssé, Lecture Notes in Physics 535, (Springer, Berlin, 2000), p. 349.
- [25] B.L. Gyorffy, J. Pindor, J.B. Staunton, G.M. Stocks, and H. Winter, J. Phys. F **15**, 1337 (1985).
- [26] H. Akai and P.H. Dederichs, Phys. Rev. B **47**, 8739 (1993).
- [27] T. Dietl, H. Ohno, F. Matsukura, J. Cibert, and D. Ferrand, Science **287**, 1019 (2000).
- [28] J. Mašek, I. Turek, V. Drchal, J. Kudrnovský, and F. Máca, Acta Phys. Polon. A **102**, 673 (2002).
- [29] A. Sakuma, J. Phys. Soc. Japan **69**, 3072 (2000).

TABLES

TABLE I. Curie temperatures [K] for the ferromagnetic state. The values \tilde{T}_c and T_c are determined from Eqs. (1) and (3), respectively. Note that the ground state for $y > 0.01$ is a partial ferromagnet.

$(\text{Ga}_{1-x}\text{Mn}_x)\text{As}$			$(\text{Ga}_{0.95-y}\text{Mn}_{0.05}\text{As}_y)\text{As}$		
x	\tilde{T}_c	T_c	y	\tilde{T}_c	T_c
0.02	281.8 K	219.6 K	0.0	346.8 K	289.2 K
0.04	332.1 K	273.4 K	0.0025	328.0 K	258.1 K
0.06	358.2 K	300.7 K	0.005	282.3 K	220.6 K
0.08	373.5 K	314.6 K	0.0075	239.5 K	176.6 K
0.10	381.9 K	320.1 K	0.01	188.2 K	125.7 K
0.12	385.3 K	319.4 K	0.0125	—	—
0.15	383.7 K	309.5 K	0.015	—	—

TABLE II. Curie temperatures [K] for the ferromagnetic state. The values T_c are determined from (3) while $T_c(n_h)$ is its rigid-band counterpart (see Sec. III C) determined for the reference Mn-concentration $x_{\text{ref}} = 0.05$. Both values coincide for the reference case of $(\text{Ga}_{0.95}\text{Mn}_{0.05})\text{As}$.

$(\text{Ga}_{1-x}\text{Mn}_x)\text{As}$			$(\text{Ga}_{0.95-y}\text{Mn}_{0.05}\text{As}_y)\text{As}$		
x	$(x_{\text{ref}}/x) T_c(n_h)$	T_c	y	$T_c(n_h)$	T_c
0.03	130 K	251 K	0.0	289 K	289 K
0.04	244 K	273 K	0.005	195 K	221 K
0.05	289 K	289 K	0.0075	142 K	177 K
0.06	285 K	301 K	0.01	79 K	126 K

FIGURES

FIG. 1. (a) The three phases in the magnetic phase diagram of $(\text{Ga}_{1-x-y}\text{Mn}_x\text{As}_y)\text{As}$. The dashed line separates n - and p -type samples. (b) The differences $E_{\text{tot}} - E_{\text{ground}}$ are plotted as a function of the order parameter r for an alloy $(\text{Ga}_{0.95-y}\text{Mn}_{x^+}\text{Mn}_{x^-}\text{As}_y)\text{As}$, $x^\pm = (1 \pm r)x/2$, $x = 0.05$, and for a set of concentrations y of As-antisites. Full circles: lattice constants of GaAs, empty circles: experimental lattice constants (for $y = 0.015$ only).

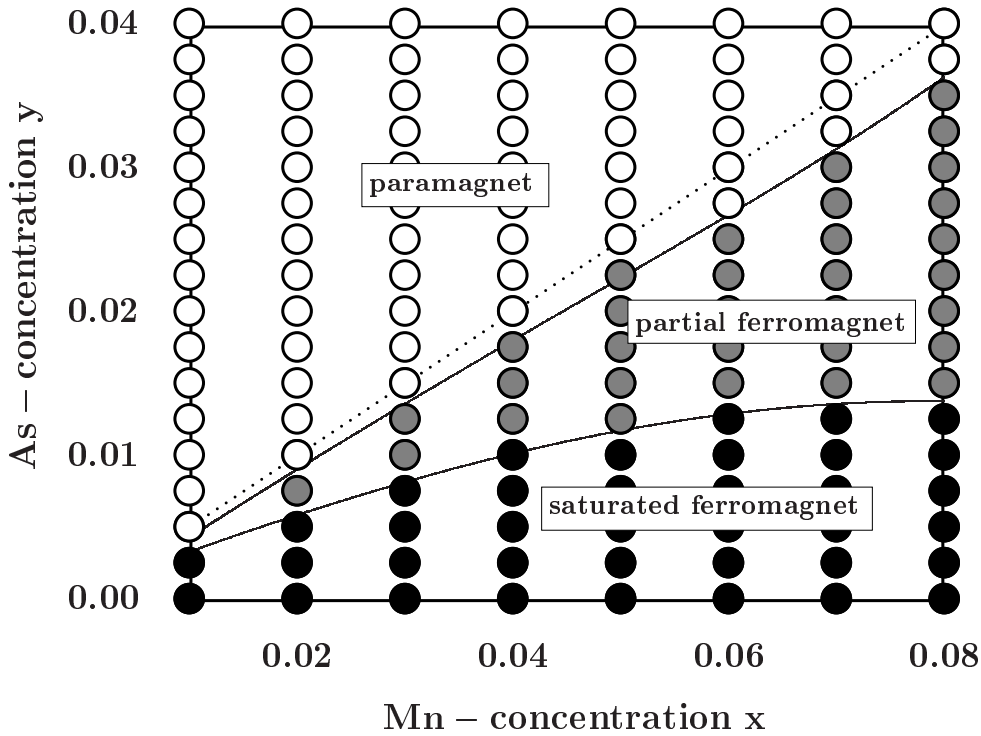


Fig. 1a

Fig. 1b

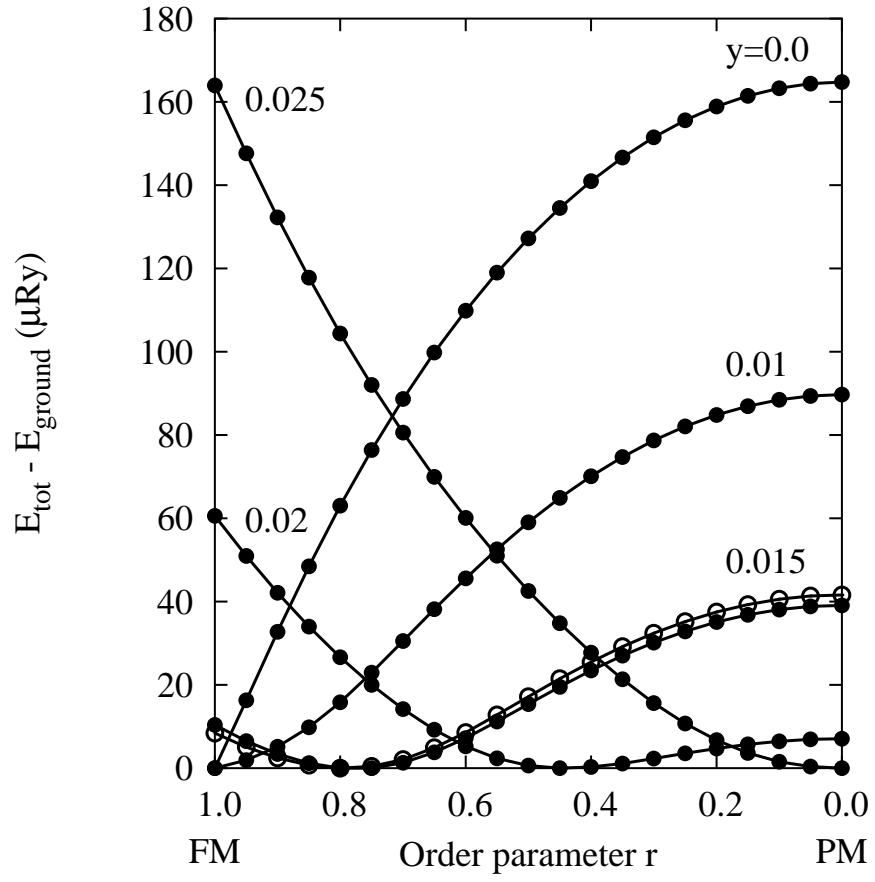


Fig. 2

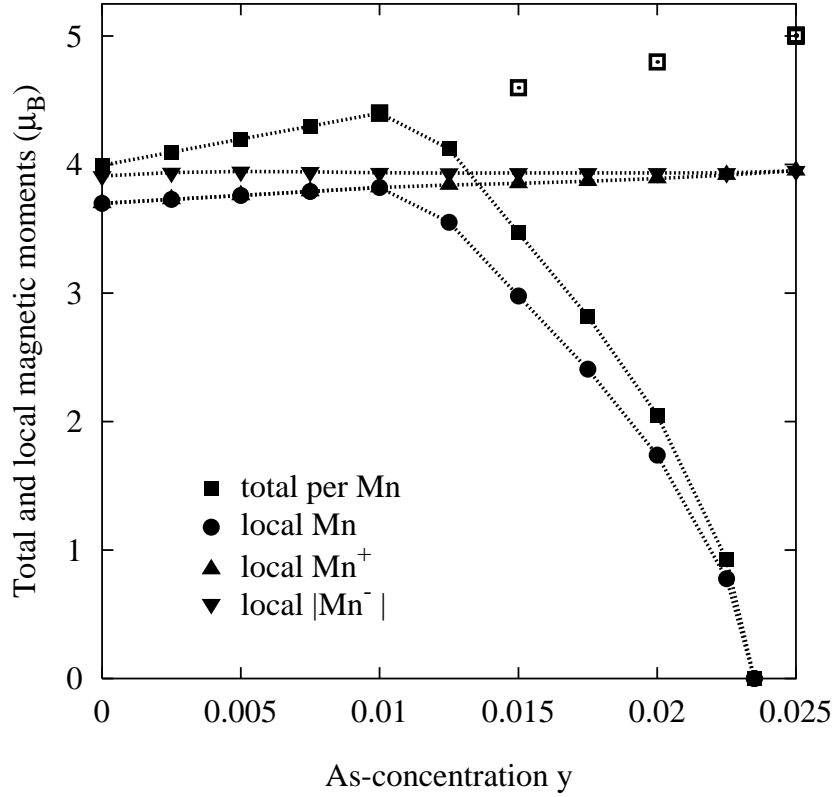


FIG. 2. Total magnetic moments and averaged local moments on Mn-atoms for $(Ga_{0.95-y}Mn_{0.05}As_y)As$ as a function of the concentration of As-antisites y . Full symbols: the ground state, empty symbols: the ferromagnetic state. Also plotted are the local moments on Mn^+ and Mn^- sites in the partial ferromagnetic state ($0.011 < y < 0.0235$). In the ferromagnetic state ($y < 0.011$) the local moments on Mn^+ -sites coincide with the local Mn-moments while the local Mn^- -moments correspond to the single-impurity limit ($x^- = 0$ in this region).

Fig. 3

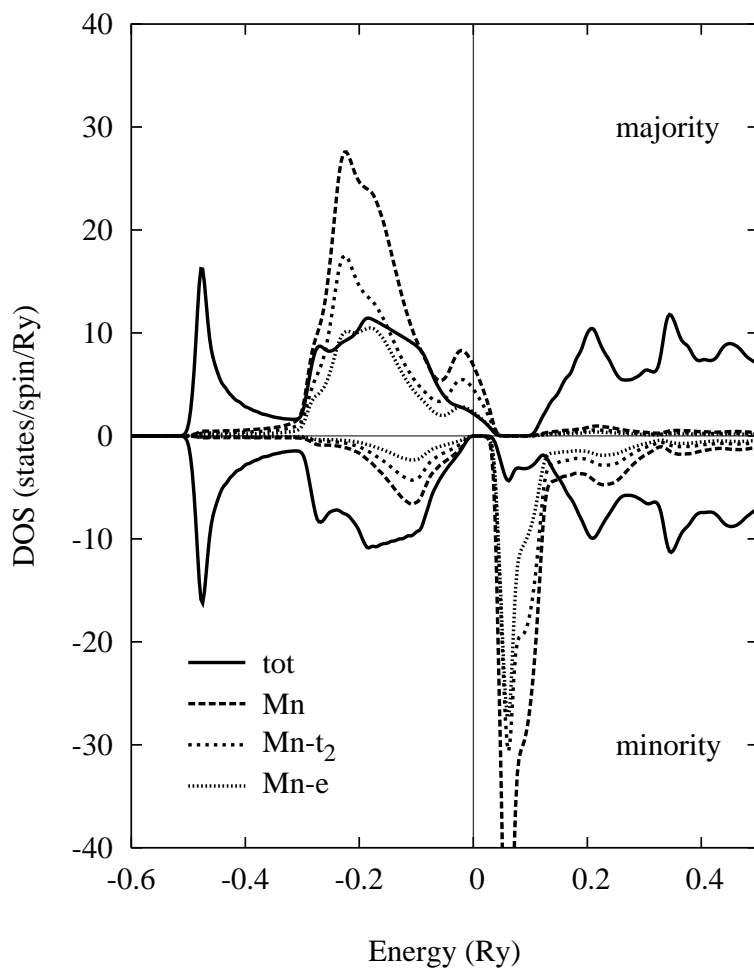


FIG. 3. Spin-dependent total densities of states and local Mn-densities of states for the Ga-sublattice in $(\text{Ga}_{0.95}\text{Mn}_{0.05})\text{As}$ as resolved with respect to the t_2 - and the e -symmetry. The Fermi level coincides with the energy zero.

Fig. 4

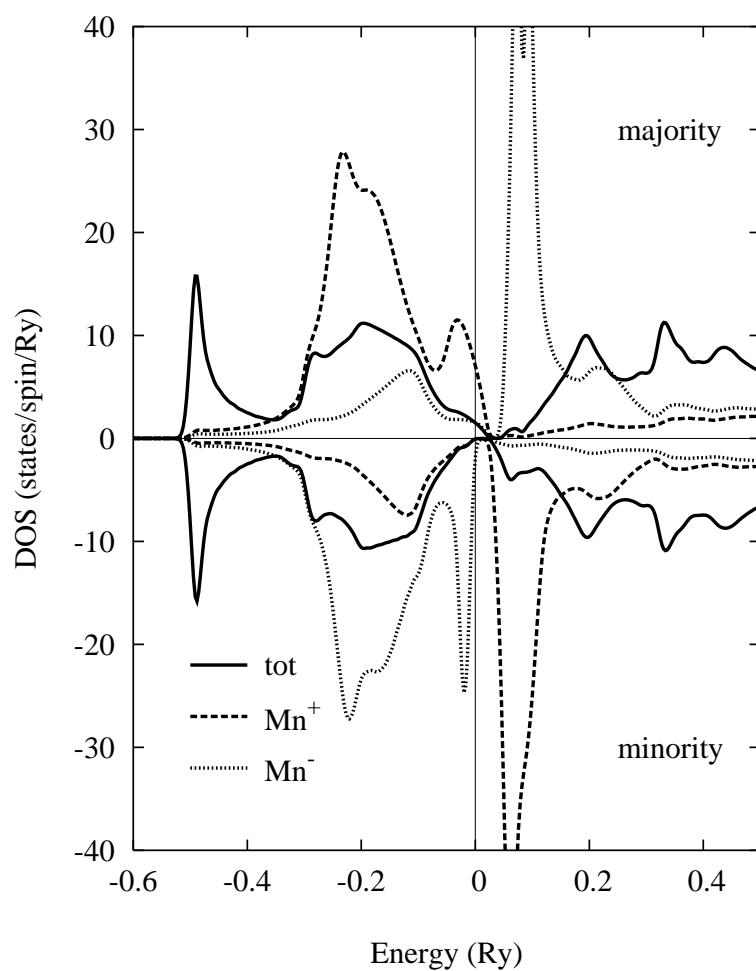


FIG. 4. Spin-dependent total densities of states and local Mn^+ - and Mn^- -densities of states for $(\text{Ga}_{0.935}\text{Mn}_{0.05}\text{As}_{0.015})\text{As}$ in the partial ferromagnetic state. The Fermi level coincides with the energy zero.

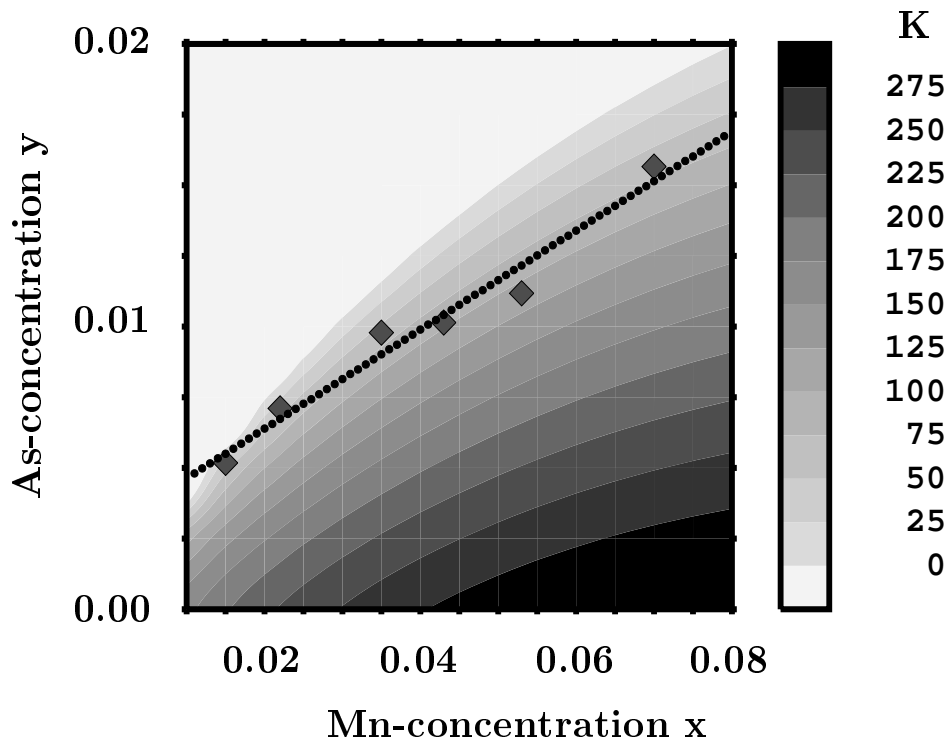


Fig. 5

FIG. 5. Contour plot of the Curie temperature as a function of the composition (x, y) assuming the ferromagnetic ground state. The symbols refer to experimental values [1] (see the text), the dotted line represents a least-square fit to these data.

Fig. 6

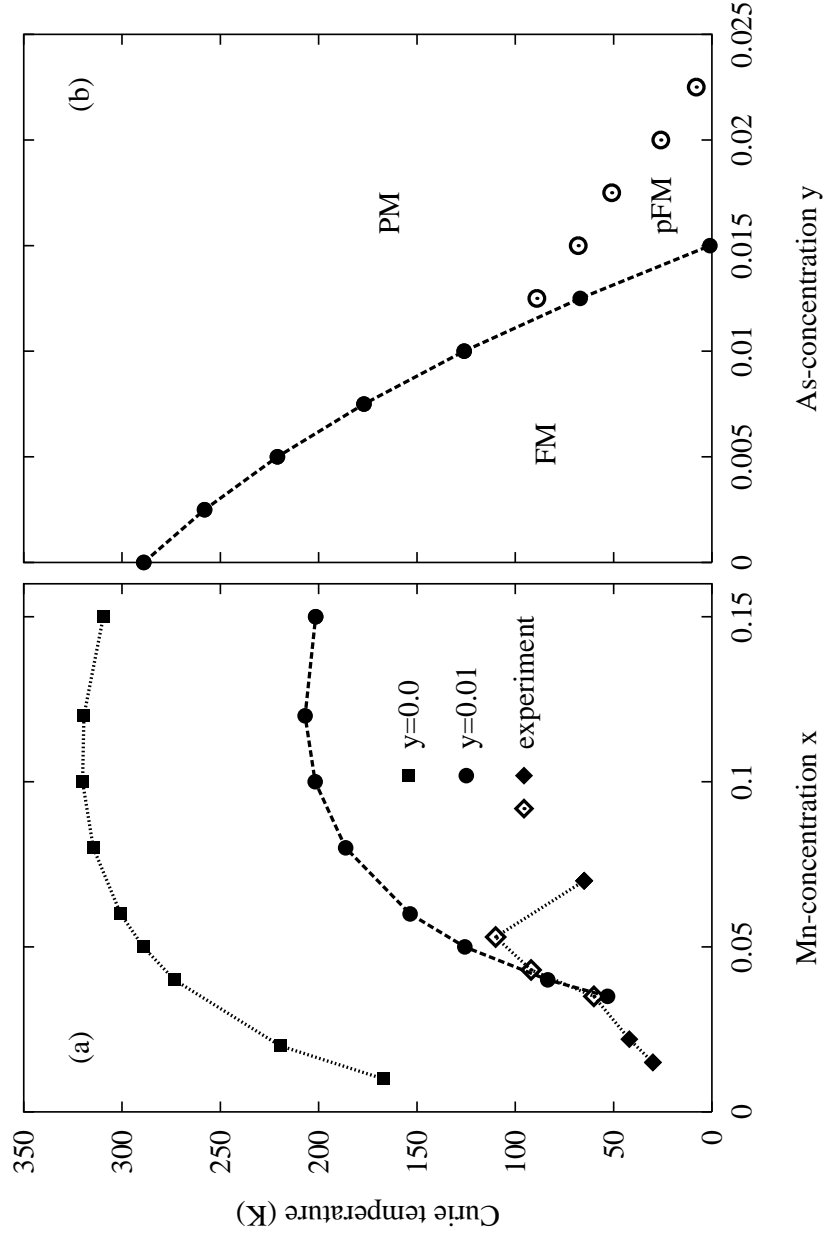


FIG. 6. (a) Curie temperatures of $(\text{Ga}_{1-x-y}\text{Mn}_x\text{As}_y)\text{As}$ in the ferromagnetic state, Eq. (3), as a function of x for $y = 0$ and $y = 0.01$ as compared to the experiment, Ref. [1] (empty diamonds: metallic ferromagnet, full diamonds: non-metallic samples); (b) Curie temperatures of $(\text{Ga}_{0.95-y}\text{Mn}_{0.05}\text{As}_y)\text{As}$ as a function of y in the ferromagnetic state, Eq. (3) (full circles) and in the partial ferromagnetic state (empty circles) which is the ground state for $y > 0.011$. The symbols FM, pFM, and PM label regions of parameters for which the ferromagnetic, partial ferromagnetic, and paramagnetic states exist, respectively.